View metadata, citation and similar papers at core.ac.uk

brought to you by CORE

provided by Repository@USM

THE EFFECTS OF ANDROGRAPHOLIDE ON THE HUMAN ORGANIC ANION TRANSPORTER 1 (hOAT1) AND PREDICTION OF ITS DRUG-HERB INTERACTION RISKS

CHONG YOONG MIN

UNIVERSITI SAINS MALAYSIA

2017

THE EFFECTS OF ANDROGRAPHOLIDE ON THE HUMAN ORGANIC ANION TRANSPORTER 1 (hOAT1) AND PREDICTION OF ITS DRUG-HERB INTERACTION RISKS

by

CHONG YOONG MIN

Thesis submitted in fulfillment of the requirements for the degree of
Master of Science

MARCH 2017

ACKNOWLEDGEMENT

I would sincerely like to express my most profound thanks to my supervisor, Assoc. Prof. Dr. Tan Mei Lan and co-supervisor Prof. Dr. Gurjeet Kaur Chatar Singh, for their encouragement, guidance and invaluable advice throughout the research period. They gave me a lot of confidence and dedicative supports along the completion of this study. Without them, the work would never have been undertaken. I would like to acknowledge MyBrain15 program for sponsoring my tuition fees in completing my Master studies. In addition, I would also like to acknowledge ScienceFund Grant and FGRS Grant for providing me financial support in completing this research project.

Special thanks to all my labmates, Tay Yea Lu, Teah Yi Fan, Noradliyanti binti Rusli and Muhammad Asyraf Abduraman, for their endless support, friendship and cares throughout the research and writing of this thesis. I am grateful for their invaluable helps and technical supports throughout the study.

Last but not least, I will be ever grateful for the unconditioned love of my family members. Thanks for their support, encouragement and above all for believing in me even when sometimes I did not believe in myself. Without them being there, this research project would never be completed.

TABLE OF CONTENTS

Acknowledgement ii

Table of Contents iii

List of Tables ix

List of Figures x

List of Abbreviations xiv

List of Symbols xix

List of Units xx

Abstrak xxii

Abstract xxiv

CHAPTER 1 – INTRODUCTION

1.1 Drug Interaction 1

  1.1.1 Drug-drug Interaction 1

  1.1.2 Drug-food Interaction 3

  1.1.3 Drug-herb Interaction 4

1.2 Pharmacokinetic and Pharmacodynamic of Drug-herb Interaction 6

1.3 Drug Transporters 9

1.4 Organic Anion Transporter (OAT) 11

1.5 Organic Anion Transporter 1 (OAT1/SLC22A6) 16

  1.5.1 Biochemistry of hOAT1 16

  1.5.2 Structure and Active Site of hOAT1 17

  1.5.3 Substrates of hOAT1 20

  1.5.4 Inhibitors of hOAT1 20

  1.5.5 Drug Interactions Involving hOAT1 24

1.6 Approaches for Assessing hOAT1-mediated Drug-herb Interaction 26
  1.6.1 Computational *in silico* Approaches 27
  1.6.2 *In vitro* Models 28
  1.6.3 *In vivo* Models 33
1.7 Herbal Compounds 35
  1.7.1 *Andrographis paniculata* 37
    1.7.1(a) Andrographolide 39
1.8 Objective of Study 43
  1.8.1 General Objectives 43
  1.8.2 Specific Objectives 43

CHAPTER 2 – MATERIALS AND METHODS

2.1 Materials and Reagents 44
2.2 Preparation of Stock and Working Solutions 46
2.3 Preparation of Glasswares and Plasticwares 47
2.4 Molecular Docking and Simulation of Ligands within the hOAT1 Active Site 47
  2.4.1 Preparation of Macromolecule File 50
  2.4.2 Preparation of Ligand File 50
  2.4.3 Grid Generation and Docking Simulation using AutoDock 4.2 51
  2.4.4 Docking Visualization and Protein-ligand Interaction Prediction 52
2.5 Cell Culture 53
  2.5.1 CHO-K1 Cell Culture 53
  2.5.2 Maintenance of Cells in Culture 53
  2.5.3 Subculturing of Cells 53

2.5.4 Preserving and Storing of Cells 54

2.5.5 Thawing of Frozen Cells 54

2.5.6 Counting Cells 54

2.6 Establishment of Recombinant CHO-hOAT1 Cell Line 55

2.6.1 Amplification of Plasmids 55

2.6.1(a) DNA Quantification 57

2.6.1(b) Restriction Enzyme Digestion 58

2.6.1(c) Agarose Gel Electrophoresis 58

2.6.1(d) DNA Sequencing 59

2.6.2 Stable Transfection and Selection of Stable Clone 59

2.6.2(a) Transfection of CHO-K1 Cell Line with hOAT1 cDNA Clone 59

2.6.2(b) Selection of Stably Transfected Clone 60

2.6.3 Trypan Blue Exclusion Test 61

2.6.4 Validation of hOAT1 Expression in CHO-K1 Cell Line 61

2.7 Quantitative Reverse Transcription Polymerase Chain Reaction (RT-qPCR) 62

2.7.1 Isolation of Total Cellular RNA 62

2.7.2 DNase Treatment of Total Cellular RNA 63

2.7.3 Electrophoresis of Total Cellular RNA on Agarose Gel 63

2.7.4 Design of Gene Specific Primers 63

2.7.5 Determination of Optimum Primer Annealing Temperature and Melt Curve Analysis 64

2.7.6 Determination of RT-qPCR Amplification Efficiency 66

2.7.7 Determination of mRNA Expression of Target Genes 66

2.8 Western Blot Analysis 67
2.8.1 Total Protein Isolation 67
2.8.2 Determination of Protein Concentration 69
2.8.3 Sodium Dodecyl Sulfate Polyacrylamide Gel Electrophoresis (SDS-PAGE) 69
2.8.4 Immunoblotting and Visualization of Protein 71
2.9 High Performance Liquid Chromatography (HPLC) Analysis 72
2.9.1 HPLC Instrumentation and Conditions 72
2.9.2 Bio-analytical Assay Validation 73
2.9.2(a) Selectivity 73
2.9.2(b) Linearity 74
2.9.2(c) Precision and Accuracy 74
2.9.2(d) Extraction Recovery 75
2.10 Uptake Transport Assay 76
2.10.1 Determination of the Optimum Incubation Time for hOAT1-mediated Uptake 78
2.10.2 Determination of K_m, V_{max} and Uptake Ratio of PAH and Andrographolide for hOAT1-mediated Uptake 78
2.10.3 Inhibition of hOAT1-mediated Uptake of PAH by Probenecid and Andrographolide 79
2.11 Cell Proliferation Assay 79
2.12 Treatment of CHO-hOAT1 cells to Determine the Effects of Probenecid and Andrographolide on the mRNA Expression and Protein Expression of Target Genes 82
2.13 Data Analysis 84

CHAPTER 3 – RESULTS

3.1 Molecular Docking of Compounds within the hOAT1 Homology Model Active Site 85

3.2 Amplification of Plasmids 92

3.3 Generation of Stably Transfected Cell Line 96

3.4 The Effect of Transfection on Cell Viability using Trypan Blue Exclusion Test 99

3.5 Validation of hOAT1 Expression in the CHO-K1 Cell Line 99

  3.5.1 Verification of mRNA Expression of hOAT1 in CHO-hOAT1 Cell Line using RT-qPCR Analysis 99

    3.5.1(a) Purity and Integrity of RNA 99

    3.5.1(b) Optimization of RT-qPCR Analysis 102

    3.5.1(c) mRNA Expression of hOAT1 Gene in the CHO-hOAT1 Cell Line 106

  3.5.2 Verification of Protein Expression of hOAT1 in CHO-hOAT1 Cell Line using Western Blot Analysis 108

3.6 HPLC Analysis 108

  3.6.1 Chromatographic Separation of Compounds 108

  3.6.2 Bio-analytical Assay Validation 112

    3.6.2(a) Selectivity 112

    3.6.2(b) Linearity 112

    3.6.2(c) Precision and Accuracy 114

    3.6.2(d) Extraction Recovery 117

3.7 Uptake Transport Assay 117

  3.7.1 Determination of the Incubation Time for hOAT1-mediated 117

Uptake
3.7.2 Determination of K_m, V_{max} and Uptake Ratio of Typical Substrate and Andrographolide for hOAT1-mediated Uptake 120
3.7.3 Effects of Probenecid and Andrographolide on Uptake Transport of PAH in CHO-hOAT1 Cells 125
3.8 The Effects of Andrographolide on Proliferation of CHO-hOAT1 cells 128
3.9 The Effects of Probenecid and Andrographolide on the mRNA Expression of Target Genes in CHO-hOAT1 Cells using RT-qPCR Analysis 128
3.10 The Effects of Probenecid and Andrographolide on the Protein Expression of Target Genes in CHO-hOAT1 Cells using Western Blot Analysis 131
3.10.1 Optimization of the Amount of Protein Used in Immunodetection 131
3.10.2 The Effects of Probenecid and Andrographolide on the Protein Expression of hOAT1 134

CHAPTER 4 – DISCUSSION 137
CHAPTER 5 – CONCLUSION 147
REFERENCES 150
LIST OF PROCEEDINGS AND PUBLICATIONS 169

LIST OF TABLES

		Page
Table 1.1	Compounds interacting with hOAT1	21
Table 2.1	List of materials and suppliers	44
Table 2.2	Stock and working solutions and their composition	46
Table 2.3	Two-dimensional (2D) structure of ligands	48
Table 2.4	RT-qPCR master mix composition	65
Table 2.5	Composition of resolving gel and stacking gel	70
Table 3.1	A summary of the molecular interactions of compounds with homology model of hOAT1	86
Table 3.2	Nucleotide sequence, optimum annealing temperature and RT-qPCR amplification efficiency of primers	103
Table 3.3	Within and between-day precision and accuracy of HPLC analysis for PAH	115
Table 3.4	Within and between-day precision and accuracy of HPLC analysis for andrographolide	116
Table 3.5	Recovery of PAH and andrographolide from cell lysate	118
Table 3.6	Uptake ratio of PAH and andrographolide at all concentration	122

LIST OF FIGURES

		Page
Figure 1.1	Predicted transmembrane topology model of OAT family	13
Figure 1.2	Model for basolateral OAT pathway	15
Figure 1.3	A three-dimensional model of hOAT1 based on the structure of GlpT	19
Figure 1.4	Decision tree to determine whether an investigational drug is a substrate for renal transporters (OCT2, OAT1 and OAT3)	31
Figure 1.5	Decision tree to determine whether an investigational drug is an inhibitor for renal transporters (OCT2, OAT1 and OAT3)	32
Figure 1.6	Morphology of *A. paniculata*	38
Figure 1.7	Chemical structure of andrographolide	40
Figure 2.1	Flowchart of molecular docking and simulation using AutoDock 4.2 software package	49
Figure 2.2	An illustration of plasmid map	56
Figure 2.3	Mathematical model for relative quantification in RT-qPCR	68
Figure 2.4	Formula used to calculate relative protein expression	83
Figure 3.1A	Molecular interactions of p-aminohippuric acid with homology model of hOAT1	87
Figure 3.1B	Molecular interactions of probenecid with homology model of hOAT1	88
Figure 3.1C	Molecular interactions of andrographolide with homology model of hOAT1	89

Figure 3.2 Agarose gel electrophoresis image to determine the size of DNA fragments following restriction enzyme digestion 93

Figure 3.3 Comparison between sequence of pCMV-Neo-hOAT1 plasmid vector against sequence in GenBank (NM_153276.2) 94

Figure 3.4 Comparison between the sequences of pCMV-Neo plasmid vector against sequences in GenBank (AF067196.1) 95

Figure 3.5 The effect of G418 sulfate on the proliferation of CHO-K1 cell line 97

Figure 3.6 Images of transfected cells after 600 µg/ml of G418 sulfate was added 98

Figure 3.7 The effect of transfection on the viability of CHO-K1 cells 100

Figure 3.8 Representative image of agarose gel electrophoresis of total RNA isolated from CHO-hOAT1 cells 101

Figure 3.9 Representative image of melt curve plots for amplification of hOAT1, ß-actin and GAPDH gene 104

Figure 3.10 Representative image of standard curve plots for amplification efficiencies of hOAT1, ß-actin and GAPDH gene 105

Figure 3.11A Fold change in gene expression of hOAT1 in CHO-hOAT1 cells relative to the cells transfected with empty plasmid vector 107

Figure 3.11B Fold change in gene expression of hOAT1 in CHO-K1 cells relative to the cells transfected with empty plasmid vector 107

Figure 3.12 Western Blot analysis for hOAT1 protein expression in the CHO-hOAT1 cells 109

Figure 3.13 HPLC/UV chromatograms of PAH 110

Figure 3.14 HPLC/UV chromatograms of andrographolide 111

Figure 3.15A Standard curve of between-day runs for six PAH concentrations ranging from 0.1 –2.5 µM 113

Figure 3.15B Standard curve of between-day runs for six andrographolide concentrations ranging from 0.125 – 2.5 µM 113

Figure 3.16 Time profile of the uptake of PAH by CHO-hOAT1 cells and cells transfected with empty plasmid vector 119

Figure 3.17A Kinetic parameters (K_m and V_{max}) determination of hOAT1-mediated uptake for PAH 121

Figure 3.17B Uptake ratio determination of hOAT1-mediated uptake for PAH 121

Figure 3.18A Kinetic parameters (K_m and V_{max}) determination of hOAT1-mediated uptake for andrographolide 124

Figure 3.18B Uptake ratio determination of hOAT1-mediated uptake for andrographolide 124

Figure 3.19 Inhibitory effect of probenecid on the uptake of PAH by CHO-hOAT1 cells 126

Figure 3.20 Inhibitory effect of andrographolide on the uptake of PAH by CHO-hOAT1 cells 127

Figure 3.21 The effect of andrographolide on CHO-hOAT1 cell proliferation 129

Figure 3.22A	The effect of probenecid on mRNA expression of hOAT1 in CHO-hOAT1 cells after 24 h incubation	130
Figure 3.22B	The effect of probenecid on mRNA expression of hOAT1 in CHO-hOAT1 cells after 48 h incubation	130
Figure 3.23A	The effect of andrographolide on mRNA expression of hOAT1 in CHO-hOAT1 cell after 24 h incubation	132
Figure 3.23B	The effect of andrographolide on mRNA expression of hOAT1 in CHO-hOAT1 cell after 48 h incubation	132
Figure 3.24	Optimization of the amount of protein used in immunodetection	133
Figure 3.25	The effect of probenecid on the protein expression of hOAT1 in CHO-hOAT1 cells	135
Figure 3.26	The effect of andrographolide on the protein expression of hOAT1 in CHO-hOAT1 cells	136

LIST OF ABBREVIATIONS

α-KG	α-ketoglutarate
% RSD	% relative standard deviation
% RE	% relative error
2D	two-dimensional
3D	three-dimensional
3D-QSAR	three-dimensional quantitative structure activity relationships
6-CF	6-carboxyfluorescein
a.a	amino acid
ABC	ATP-binding cassette
ACTB	ß-actin
ADT	AutoDock Tools
APS	ammonium persulphate
Ala	alanine
Arg	arginine
Asp	aspartate
BCRP	breast cancer resistance protein
BSA	bovine serum albumin
cDNA	complementary deoxyribonucleic acid
cGMP	cyclic guanosine monophosphate
CHM	Chinese herbal medicines
CHO-K1	Chinese hamster ovary
CO_2	carbon dioxide
C_q	quantification cycle
CYP3A4	cytochrome P450 3A4 isoenzyme

DDI	drug-drug interaction
DMSO	dimethylsulfoxide
EMA	European Medicines Agency
EPPs	Entry Point Projects
ETP	Economic Transformation Programme
FBS	fetal bovine serum
FDA	United States Food and Drug Administration
FEB	free energy of binding
GI_{50}	growth inhibition
GlpT	glycerol 3-phosphate
GZ	Gui Zhi Fu Ling Wan
HBSS	Hank’s balance salt solution
HCl	hydrochloric acid
HEK293	human embryonic kidney
HEPES	4-(2-hydroxyethyl)-1-piperazineethanesulfonic acid
HR2	histamine receptor 2
HIV	human immunodeficiency virus
hOAT1	human organic anion transporter 1
hOAT2	human organic anion transporter 2
hOAT3	human organic anion transporter 3
hOAT4	human organic anion transporter 4
hOAT10	human organic anion transporter 10
HPLC	high performance liquid chromatography
hURAT1	human urate transporter 1
IC_{50}	half-maximal inhibitory concentration

Ile	isoleucine
K^+	potassium
K_i	inhibition constant
K_m	Michaelis-Menten constant
LacY	lactose permease
LC_{50}	lethal concentration
LC-MS/MS	liquid chromatography-tandem mass spectrometry
LGA	Lamarckian genetic algorithm
LLOQ	lower limit of quantification
Lys	lysine
MDCK	Mardin-Darby canine kidney
Met	methionine
MFS	major facilitator superfamily
MM	Michaelis-Menten
mOAT1	mouse organic anion transporter 1
mOAT3	mouse organic anion transporter 2
mRNA	messenger ribonucleic acid
MRP	multidrug resistance protein
Na^+	sodium
NKEAs	National Key Economic Areas
NSAIDs	nonsteroidal anti-inflammatory drugs
OA^-	organic anion
OATs	organic anion transporters
OAT1	organic anion transporter 1
OAT3	organic anion transporter 3

OATP	organic anion transporting polypeptide
OATP1B1	organic anion transporting polypeptide 1B1
OATP1B3	organic anion transporting polypeptide 1B3
OCTs	organic cation transporters
OCT2	organic cation transporter 2
P-gp	P-glycoprotein
PAH	p-aminohippuric acid
PBS	phosphate buffer saline
PGE_2	prostaglandin E_2
Phe	phenylalaline
R^2	correlation coefficient
RIPA	radioimmunoprecipitation assay
RT-qPCR	quantitative reverse transcription polymerase chain reaction
RMSD	root mean square deviation
rOAT1	rat organic anion transporter 1
SD	standard deviation
SDS	sodium dodecyl sulfate
SEM	standard error of the mean
Ser	Serine
SLC	solute carrier
SLC22A	solute carrier transporters family 22A
S.O.C	super optimal broth with catabolite repression
SSRIs	selective serotonin reuptake inhibitors
TBE	Tris-Borate EDTA
TCAM	traditional complementary and alternative medicine

TEMED	tetramethylethylenediamine
TFA	trifluoroacetic acid
TGI	total growth inhibition
Tyr	tyrosine
UV	ultraviolet
Val	valine
V_{max}	maximal velocity
v/v	volume per volume
WHO	World Health Organization
w/v	weight per volume

LIST OF SYMBOLS

α	alpha
~	approximately
*	asterisk
ß	beta
–	dash
=	equals
>	greater than
-	hyphen
λ	lamda
<	less than
≤	less than or equal to
/	or
±	plus or minus
®	registered trademark
x	times
™	trade mark
π	Pi

LIST OF UNITS

%	percentage
°C	degree Celcius
Å	Ångström
bp	base pair
cells/ml	cells per milliliter
g	gram
g/mol	gram per mole
h	hour
kb	kilobyte
kDa	kiloDalton
M	molar
min	minute
ml	milliliter
ml/min	milliliter per minute
mm	millimeter
mM	millimolar
ms	millisecond
ng	nanogram
ng/ul	nanogram per microliter
nm	nanometer
nmol/mg	nanomole per milligram
N	normality
pmol/min/mg	picomole per minute per milligram
rpm	revolutions per minute

psi	pounds per square inch
s	second
U/ml	unit per milliliter
μg	microgram
μg/ml	microgram per milliliter
μl	microliter
μm	micrometer
μM	micromolar
V	volt

KESAN ANDROGRAPHOLIDE KE ATAS PENGANGKUT ANION ORGANIK MANUSIA 1 (hOAT1) DAN RAMALAN RISIKO INTERAKSI UBAT-HERBA

ABSTRAK

Kepentingan dalam penggunaan ubat-ubatan berasaskan herba dan produk herba telah berkembang dengan pesat di seluruh dunia. Kefahaman mengenai potensi ke atas interaksi herba dan perubatan moden telah meningkat disebabkan populariti kandungan herba. Pengangkut ubat telah diiktiraf memainkan peranan utama dalam penyerapan, pengedaran, metabolisme dan penyingkiran ubat. Oleh sebab itu, interaksi antara ubat-ubatan dan pengangkut boleh berlaku. Pengangkut anion organik manusia 1 (hOAT1) memainkan peranan penting dalam pengedaran dan penghapusan pelbagai bahan dalaman dan xenobiotik. Hempedu bumi telah digunakan secara meluas untuk merawat selesema, cirit-birit, radang dan jangkitan saluran pernafasan. Dalam kajian ini, andrographolide merupakan sebatian bioaktif utama daripada hempedu bumi dan kesannya ke atas aktiviti pengambilan hOAT1 telah dinilaikan. Sel rekombinan CHO-K1 dengan ekspresi hOAT1 secara stabil (sel CHO-hOAT1) telah dihasilkan untuk mengkaji aktiviti pengangkutan hOAT1. Ekspresi hOAT1 dalam sel CHO-hOAT1 telah disahkan dengan menggunakan analisis RT-qPCR dan Western blot. Aktiviti pengambilan hOAT1 telah dijalankan untuk menentukan sama ada andrographolide adalah substrat atau perencat kepada hOAT1. Hasil kajian menunjukkan bahawa nisbah pengambilan andrographolide adalah 1.208 dan menunjukkan bahawa andrographolide tidak mungkin sebagai substrat kepada hOAT1. Andrographolide juga tidak mungkin adalah perencat kepada hOAT1 disebabkan nilai IC_{50} andrographolide tidak dapat ditentukan pada kepekatan tertinggi yang diuji. Di samping itu, andrographolide tidak menunjukkan sebarang perubahan ketara pada mRNA dan protein hOAT1 dalam sel CHO-hOAT1. Kesimpulannya, andrographolide bukan merupakan substrat, perencat dan pencetus kepada hOAT1.

THE EFFECTS OF ANDROGRAPHOLIDE ON THE HUMAN ORGANIC ANION TRANSPORTER 1 (hOAT1) AND PREDICTION OF ITS DRUG-HERB INTERACTION RISKS

ABSTRACT

Interest in the use of medicinal herbs and herbal products has grown rapidly throughout the world. The popularity of herbal constituents makes it important to understand potential interactions between herbs and modern medicine. Drug transporters have been recognized to play a major role in drug absorption, distribution, metabolism and elimination and hence, clinically significant transporter-mediated drug interactions can occur. Human organic anion transporter 1 (hOAT1) plays a key role in the distribution and elimination of a variety of endogenous substance and xenobiotics. *Andrographis paniculata* Nees has been widely used for treating common colds, diarrhea, inflammation and upper respiratory tract infections. In this study, andrographolide, a major bioactive compound isolated from *A. paniculata* Nees, was evaluated for its effects on hOAT1-mediated uptake. Recombinant CHO-K1 cell line stably expressing hOAT1 (CHO-hOAT1 cells) was established to carry out hOAT1-mediated uptake transport activity. The expression of hOAT1 in CHO-hOAT1 cells was confirmed by RT-qPCR and Western blot analysis. The uptake transport assay was used to determine if andrographolide is a substrate or inhibitor of hOAT1. The results showed that the uptake ratio of andrographolide was 1.208, indicating that andrographolide is unlikely to be a substrate of hOAT1. Andrographolide is also unlikely an inhibitor of hOAT1 as the IC_{50} value of andrographolide was not determined at the highest concentration tested. In addition, andrographolide did not exhibit any significant changes on mRNA and protein expression of hOAT1 in the

CHO-hOAT1 cells. In conclusion, andrographolide is unlikely to be a substrate, inhibitor or inducer for hOAT1.

CHAPTER 1

INTRODUCTION

1.1 Drug interaction

A drug interaction is a situation in which the disposition of one drug is altered by another when both are administered together (Mick, 2005). Drug interactions can range in severity from theoretical to clinically significant, sometimes prolonging morbidity and even death. However, benefit may be obtained from drug interactions that increase drug exposure, improve therapeutic outcome and minimize side effects (Piscitelli and Rodvold, 2005). Drug interactions occur not only with other drugs, but also with herbal supplements and food, leading to drug-herb interactions and drug-food interactions respectively.

1.1.1 Drug- drug interaction

As large number of drugs are introduced every year, drug-drug interactions become an important aspect of drug development, especially for safety (Manzi and Shannon, 2005). Drug-drug interactions (DDI) can cause profound clinical effects, either by reducing therapeutic efficacy or enhancing toxicity of drugs. Drug-drug interaction is one of the main cause for drug withdrawal from the market (Huang *et al.*, 2008). Mibefradil, a drug used to treat high blood pressure or chest pain, has been withdrawn from U.S market due to its interaction with others drugs. It has been implicated in various case reports as interacting with cyclosporine, statins and cisapride; in some cases, renal failure and torsades de pointes were reported (Qureshi *et al.*, 2011). Similarly, cases of torsades de pointes have been reported when cisapride was administered with other drugs that inhibited cytochrome P450 3A4 isoenzyme (CYP3A4) (Yaffe and Aranda, 2010). Cisapride was removed from the U.S. market in 2000 (Wynn *et al.*, 2009).

With the seemingly constant flow of new therapeutic drugs and new treatment indications for existing medications, polypharmacy is increasingly common, especially among elderly patients (Lin, 2003). Polypharmacy is defined as concurrent use of multiple drugs in one prescription. As the number of medications taken by a given patient increases, so does the risk of drug interactions. The risk of drug interactions is speculated to increase from approximately 6% in patients taking only two medications to 50% in those taking five medications and 100% in those taking ten medications (Johnson *et al.,* 1994). Concomitant use of antibiotics among warfarin users are associated with a high risk of overanticoagulation (Juurlink, 2007). In this case, antibiotic medications (quinolones, sulfonamides and azole antifungals) interact with warfarin and increase the risk of major bleeding through disruption of intestinal flora that synthesize vitamin K, and inhibition of CYP isoenzymes which metabolize warfarin (Juurlink, 2007; Schelleman *et al.,* 2008).

While recognition of adverse drug-drug interactions is important, the recognition and appropriate use of beneficial drug-drug interactions is equally important task in clinical practice (Yadav, 2008). The use of ritonavir to enhance blood concentrations of other protease inhibitors in antiretroviral treatment of human immunodeficiency virus (HIV) is an example of a beneficial drug-drug interaction that provides enhanced viral suppression (Zeldin and Petruschke, 2004).

Therefore, the potential for interactions with medications should always be considered when administering or prescribing any drug. With new drugs entering the market at a rapid pace, identification of new clinically significant drug interactions is essential.

1.1.2 Drug-food interaction

A food-drug interaction occurs when a food, or one of its active ingredients, interferes with the way a drug acts in the human body (Bobroff *et al.*, 2009). Diet and lifestyle can sometimes have a significant effect on how drugs behave in the human body. These interactions may occur out of accidental misuses or due to lack of knowledge about the active constituents found in the food. The main cause of clinically relevant food-drug interactions is food-induced changes in the bioavailability of the drug (Bushra *et al.*, 2011).

Food-drug interaction is a common hidden problem encountered in clinical practice. Food intake can influence the effectiveness of an antibiotic, one of the drugs that are widely prescribed in medical practice. Co-administration of ciprofloxacin with milk products which are rich sources of divalent ions, such as calcium and magnesium decrease the absorption of ciprofloxacin (Papai *et al.*, 2010). In addition, eating some vegetables that high in Vitamin K such as broccoli, asparagus, kale and parsley can interfere with the effectiveness and safety of warfarin therapy (Bushra *et al.*, 2011).

Several fruits and berries such as grapefruit, sevillian orange, pomelo and star fruit contain furanocoumarins that inhibit CYP3A4 enzymes, which plays important role in drug metabolism (Molden and Spigset, 2007). A number of studies have documented that furanocoumarins present in grape fruit juice increase the oral bioavailability of medications which are CYP3A4 substrates like felodipine, midazolam, and cyclosporine and resulted in their concentrations to increase to toxic levels (deCastro *et al.*, 2007). The *in vitro* data also suggest that compounds present in grapefruit juice are also inhibitors of drug transporters such as P-glycoprotein (P-gp) and organic-anion transporting polypeptide (OATP) (Dresser *et al.*, 2002; deCastro *et al.*, 2007).

Food-drug interactions may influence the safety and efficacy of drug therapy, as well in the nutritional status of the patient. Therefore, it is recommended that patients should ask for advice from doctors and pharmacists about their food intake so that such interactions can be avoided.

1.1.3 Drug-herb interaction

Interest in the use of medicinal herbs and herbal products has grown rapidly throughout the world (Kim *et al.*, 2013). According to the World Health Organization (WHO), about 70% to 80% of the world population relies mainly on herbal medicine for their primary health care (WHO, 2000). Herbal medicine usage is not only popular among individuals, but also among primary health care provider in some developing countries.

The popularity of herbal medicine makes it important to understand potential interactions between such properties and prescribed drugs. Drug-herb interactions refer to the possibility that some herbal constituents may alter the pharmacologic effects of conventional drug given concurrently, or vice versa. The results may be either enhanced or reduced drug or herb effects, or the appearance of a new effect that is not anticipated from use of the drug or herb alone (Wynn and Fougere, 2007). The likelihood of drug-herb interactions could be higher than drug-drug interactions, simply because drugs usually contain single chemical entities, while herbal preparations contain a mixture of pharmacologically active constituents (Fugh-Berman and Ernst, 2001).

Drug-herb interaction is one of the most important clinical consequences and has been reported in various case reports (Fasinu *et al.,* 2012). Several herbal medicines have been reported for their adverse drug reactions and interactions with prescription medications. *Ginkgo biloba*, one of the popular traditional Chinese medicines has been reported for its possible interaction with aspirin, ibuprofen and warfarin resulting in spontaneous bleeding (Chavez *et al.,* 2006). Based on preliminary studies, ginseng, a staple Chinese medicine, may increase the risk for hypoglycemia. Therefore, concurrent use of ginseng with anti-diabetic medication may increase the risk for hypoglycemia (Chavez *et al.*, 2006). Ginseng product which contained germanium may have resulted in the interaction with furosemide as concomitant use of ginseng and furosemide has been shown to decrease the diuretic effects of furosemide (Becker *et al.,* 1996). St. John's wort, also known as *Hypericum perforatum,* is one of the most extensively studied herbal products. Concurrent use of St. John's wort with serotonin selective re-uptake inhibitors and other antidepressants may increase the risk for serotonin syndrome and other central nervous system reactions (Chavez *et al.*, 2006). Case reports of likely or possible serotonin syndrome associated with use of St. John wort have been reported with buspirone, loperamide, nefazodone, paroxetine, sertraline and venlaxafine (Fugh-Berman and Ernst, 2001).

While drug-herb interactions become more prevalent and reports of adverse effects continue to increase, the guidelines for toxicity evaluation and scheduling of herbal medicines are lacking. United States Food and Drug Administration (FDA) mandate that only medicines have to be proven to be safe before being released to the market (Zamri, 2014). Herbal products which are classified as dietary supplements are not regulated as medicines by the FDA as long it is not marketed under the indication of preventing diseases. In many cases herbal products can be marketed without providing evidence of safety or efficacy. As such, more clinically relevant research is required in this area as current information on drug-herb interaction is insufficient for clinical application (Fasinu *et al.*, 2012).

1.2 Pharmacokinetic and pharmacodynamic of drug-herb interaction

In terms of mechanisms, drug interactions can be broadly categorized as either pharmacodynamic or pharmacokinetic-based interaction. Pharmacodynamic interactions refers to interactions in which drugs influence each other's effects directly (Cascorbi, 2012). Pharmacodynamic interactions may occur when a drug has either additive or antagonist effect in relation to another drug. The underlying mechanisms include competition at molecular or cellular sites of action. An additive effect occurs when selective serotonin reuptake inhibitors (SSRIs) such as citalopram are taken simultanueously with nonsteroidal anti-inflammatory drugs (NSAIDs) (Andrade *et al.*, 2010). SSRIs inhibit the transport of serotonin into the platelets, leading to further impairment of function and enhancing the risk of upper gastrointestinal bleeding. The risk of SSRI-associated upper gastrointestinal bleeding is further increased with the concurrent use of NSAIDs including aspirin and ibuprofen. Conversely, antagonist effect occurs when drugs with opposing effects reduce the response to one or both drugs. NSAIDs (ibuprofen and piroxicam) which tend to increase blood pressure may inhibit the antihypertensive effect of drugs such as ACE inhibitors if both drugs prescribed together at the same time (Pavlicevic *et al.*, 2008).

Pharmacokinetic interactions result from an alteration of the absorption, distribution, metabolism and elimination processes of a drug substance by another compound when they are given concomitantly (Zhang *et al.*, 2009). The risks of pharmacokinetic drug interaction includes two major adverse drug effects namely, pharmacotoxicity and treatment failure. Pharmacokinetic interactions have been the main focus for both the FDA and European Medicines Agency (EMA) guidelines (Prueksaritanont *et al.*, 2013).

Absorption is the entry of drug substances into the systemic circulation via various ways such as the mucous membranes of the gut or lungs, the skin, or from the site of an injection (Baynes and Hodgson, 2004). Absorption of two drugs at or around the same time may result in clinically significant drug interactions. Antibiotics such as the fluoroquinolones and tetracyclines will bind to iron, calcium and magnesium in antacids if given simultaneously (Yadav and Yadav, 2008). The concurrent use of these compounds result in treatment failure and the emergence of resistant organisms as the antibiotics will be excreted with little or no systemic absorption of the antibiotics (Manzi and Shannon, 2005).

Following absorption into the systemic circulation, the drug is distributed throughout the body. Distribution of drugs depend on total body water, extracellular fluid, percentage of adipose tissue and plasma protein binding (Manzi and Shannon, 2005). Drug interactions affecting distribution include competition for the binding sites on plasma protein (Patsalos and Perucca, 2003). According to a case report published by Carvalho and co-workers, a 12 years old patient with refractory epilepsy syndrome was presented with phenytoin toxicity, following a concomitant treatment with both phenytoin and valproic acid (Carvalho *et al.*, 2014). Concurrent use of phenytoin with valproic acid increases the free fraction of phenytoin due to competition for the same binding sites. The high level of free fraction of phenytoin eventually increases the toxicity of phenytoin (Troy, 2006).

Metabolism is the enzymatic conversion of a drug into more water soluble metabolites that are suitable for excretion through the kidneys. Most of the drug metabolism processes occur in the liver (Troy, 2006). Drug metabolism is divided into 2 phases, namely, phase I and phase II reactions. Phase I reactions include the processes of oxidation, hydrolysis and reduction, resulting in a compound that is generally less toxic and more hydrophilic (Manzi and Shannon, 2005). On the other hand, phase II reactions include glucuronidation, sulfation, acetylation and methylation, primarily result in the termination of biologic activity of the drug (Gibson and Skett, 2001). In fact, most of drug interactions occurring during metabolism are the result of inhibition or induction of CYP enzymes (Palleria *et al.*, 2013). The CYP enzymes are unique isoenzymes found primarily in the liver and are responsible for the metabolism process of many drugs and toxins. Concurrent drug therapy can inhibit drug-metabolizing enzymes and result in toxicity. Erythromycin is a macrolide antibiotic and has been reported cause drug interactions when prescribed with statin (atorvastatin and simvastatin) (Becker, 2011). Erythromycin inhibits the activity of CYP3A4 and thus, raises the plasma level of statins which are metabolized by CYP3A4. This potential drug interaction eventually increases the toxicity of statins. In a case report, a 70 years old man developed myalgia and fatal rhadomyolysis after receiving concomitant treatment of erythromycin and simvastatin (Dubash *et al.*, 2010).

Elimination is the excretion of drug molecules from the body, usually by removal of the parent drug or metabolites through the kidney (Lee *et al.*, 2006). Renal elimination can be affected by any drugs that affect glomerular filtration rate, tubular secretion and tubular reabsorption (Bonate and Howard, 2005). Drug interactions can inhibit renal tubular secretion and assist in maintaining a higher serum concentration than the body would normally allow (Yaffe and Aranda, 2010). A notable example of this drug interaction, used long ago intentionally for therapeutic benefit, is the combination of probenecid and penicillin to increase antibiotic serum concentrations (Piscitelli and Rodvold, 2005). In the kidney, probenecid reduces the active tubular secretion of penicillin by inhibiting organic anion transporters (OATs) in the basolateral membrane of the proximal tubular cells. Thus, the clearance of penicillin will be reduced leading to an increase in plasma concentration and extending half-lilfe of penicillin (Cunningham *et al.*, 1981). This effect is exploited therapeutically in the treatment of infections.

Effects of one drug on the absorption, distribution, metabolism or excretion of another drug may lead to change in exposure leading to altered response and caused numerous drug interactions have been identified. Thus, pharmacokinetic drug interaction is recognized as an important consideration in drug development and regulatory review.

1.3 Drug transporters

Evaluation of a new chemical entity's drug-drug interaction potential is an integral part of drug development and regulatory review prior to its market approval (Zhang *et al.*, 2006). To date, CYP-mediated drug interactions have been suggested as a critical first step in the assessment of drug interactions and are now widely accepted by the pharmaceutical industry (FDA, 2012). In addition to the effects of drug metabolizing enzymes on the pharmacokinetic drug interactions, there is an increasing recognition that transporters play an important role in modulating drug absorption, distribution, metabolism and elimination (Zhang *et al.*, 2009). Clinical pharmacokinetic drug-drug interaction studies have suggested that transporters often work together with drug metabolizing enzymes in drug absorption and elimination (Giacomini *et al.*, 2010).

Functionally, transporters can be classified into two major superfamilies namely, the ATP-binding cassette (ABC) family transporters and solute carrier (SLC) family transporters. ABC transporters include P-glycoprotein (P-gp), multidrug resistance protein (MRP) and breast cancer resistance protein (BCRP) are efflux transporters which bind to ATP and use the energy to drive the transport of various drugs across the plasma membrane (Konig *et al.*, 2013). SLC transporters such as organic anion transporting polypeptides (OATPs), organic anion transporters (OATs) and organic cation transporters (OCTs) are responsible to mediate the flow of various drugs over the cell membrane ranging from the cellular uptake to the absorption of drugs (Roth *et al.*, 2012). Both ABC and SLC transporters determine plasma and concentration of a broad variety of drugs. Transporters are expressed in the small intestine, liver and kidney, particularly important in drug disposition and drug-drug interactions (Muller and Fromm, 2011). Transporters expressed in blood-tissue barrier have been shown to protect sensitive tissues from potentially toxic compounds (Konig *et al.*, 2013).

The major underlying mechanism of transporter-based drug interactions may be inhibitory, inductive or both. Such transporter-based interactions will be clinically significant if elimination of the affected drug or the distribution into a target tissue is mediated primarily by the transporter and that the interaction results in the concentration of the affected drug at the site of action or toxicity to fall outside of the therapeutic range (Endres *et al.*, 2006). Furthermore, transporter-based interactions may affect the concentration of the substrate in a particular tissue without altering the blood or plasma concentration of the substrate. Interactions occurring at the blood-brain barrier do not affect the drug exposure in the circulating blood but only the pharmacological and/or toxicological effect of the drug (Marzolini *et al.*, 2011) . Cyclosporine A, an inhibitor of P-gp affected the distribution of verapamil, a P-gp substrate into the brain by inhibiting P-gp efflux, without significantly affecting the plasma or blood concentration of the verapamil (Sasongko *et al.*, 2005). This is possible because the amount of drug distributing into the brain is only a small fraction of the total amount of the drug in the body. Sometimes, transporter-based drug interactions lead to beneficial effect instead of clinical consequences. Co-administration of probenecid with cidofovir reduced the nephrotoxicity of cidofovir due to inhibition of human organic anion transport (hOAT) of cidofovir into the kidney epithelial cells by probenecid (Endres *et al.*, 2006).

As transporter-mediated drug interactions are being increasingly identified, it is important to predict transporter-based drug interactions for evaluation in the drug discovery and development process. Thus, FDA and EMA guideline on the investigation of drug interactions provides recommendations on the seven most relevant drug transporters, namely P-gp, BCRP, organic anion transporting polypeptide 1B1 (OATP1B1), OATP1B3, organic anion transporter 1 (OAT1), OAT3 and organic cation transporter 2 (OCT2) (FDA, 2012).

1.4 Organic anion transporter (OAT)

Among the transporters, organic anion transporters (OATs), which belong to the amphiphilic solute carrier transporters family 22A (SLC22A), are key determinants in the absorption, distribution and elimination of a diverse array of exogenous and endogenous compounds (Sweet, 2005). OATs are characterized by broad substrate specificity and the ability to interact with a wide variety of compounds that are not only small, amphiphilic organic anions but also uncharged molecules and even some organic cations (Riedmaier *et al.*, 2012). OATs interact with many clinically relevant and commonly prescribed anionic drugs including β–lactam antibiotics, diuretics, anti-cancer drugs, NSAIDs, and anti-HIV therapeutics (Sekine *et al.*, 2000). As a consequence of the multi-specific substrate recognition of the transporter, clinically significant transporter-mediated drug interactions can occur. Drugs in the plasma may compete for the transporter processes, thus mutually influencing each other's pharmacological and toxicological profile (Duan *et al.*, 2012).

Cloned OATs have several common structural features including 12 transmembrane domains flanked by intracellular amino- and carboxyl termini. A cluster of potential glycosylation sites localized in the first extracellular loop between transmembrane domains 1 and 2, and multiple phosphorylation sites present in the intracellular loop between transmembrane domains 6 and 7 and in the carboxyl terminus. Figure 1.1 shows the predicted transmembrane topology model of OAT family.

To date, several members of the OAT family have been identified, which differ from each other by their localization, expression level and substrate specificity. In human kidney, human organic anion transporter 1 (hOAT1/SLC22A6), hOAT2 (SLC22A7) and hOAT3 (SLC22A8) are localized in the basolateral membrane, and hOAT4 (SLC22A11), hOAT10 (SLC22A13) and human urate transpoter 1 (hURAT1/SLC22A12) are found in the apical cell membrane of proximal tubule cells, respectively. Among OATs, mRNA levels of hOAT1 and hOAT3 were much higher than those of other organic ion transporters in the human kidney cortex (Motohashi *et al.*, 2002). In addition, many previous studies have reported that hOAT1 and hOAT3

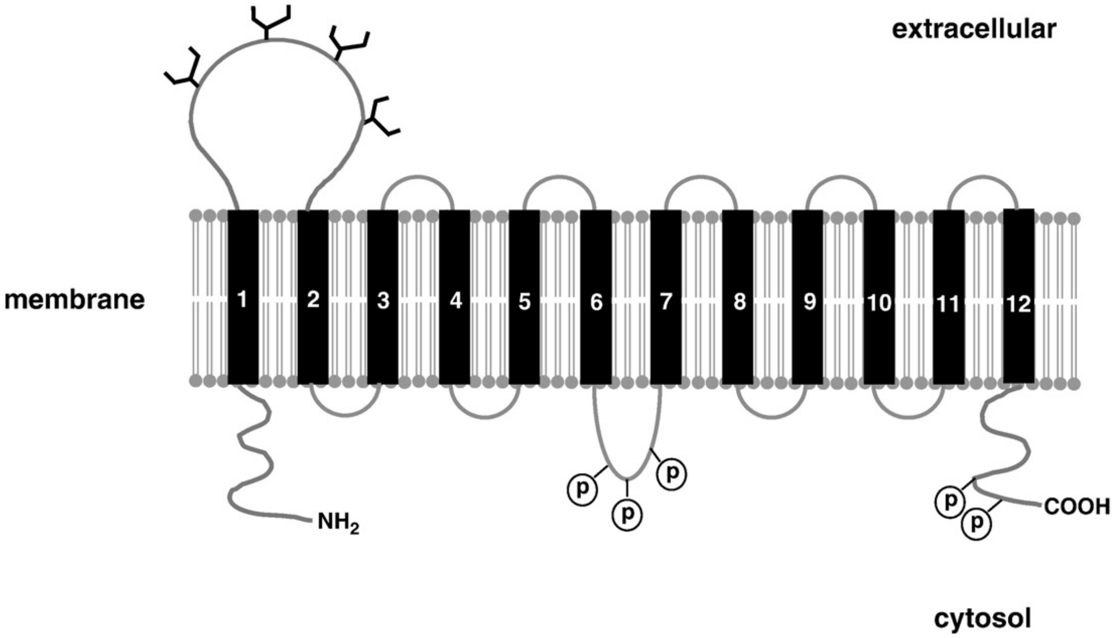
extracellular
membrane
1
2
3
4
5
6
7
8
9
10
11
12
p
p
p
p
p
NH2
COOH
cytosol

Figure 1.1 Predicted transmembrane topology model of OAT family. Twelve transmembrane domains are numbered from 1-12. Potential glycosylation sites are denoted by tree-like structures and phosphorylation sites are labeled as “P”. [Adapted from: Duan and You, 2010]

actively mediated tubular uptake of various therapeutics (Robertson and Rankin, 2006). Modulators of hOAT1 and hOAT3 activities are known to have high potential for drug interactions in the combination therapy and alter the pharmacokinetics of various drugs particularly that are eliminated from the body mainly via urinary excretion (Konig *et al.*, 2013).

In the kidney, hOAT1 and hOAT3 mediate a tertiary transport mechanism to move organic anions across the basolateral membrane into the proximal tubule cells for subsequent exit across the apical membrane into the urine for excretion (Duan and You, 2010). Through this tertiary transport mechanism, Na^+/K^+-ATPase maintains an inwardly directed Na^+ gradient from blood to cell. The Na^+ gradient then drives a sodium dicarboxylate cotranspoter, sustaining an outwardly directed dicarboxylate gradient that is utilized by hOAT1, hOAT3 or both, to move the organic anion substrates into the cell. This process indirectly links organic anion transport to metabolic energy and the Na^+ gradient, allowing the entry of a negatively charged substrate against both its chemical concentration gradient and the electrical potential of cell (Duan and You, 2010). Figure 1.2 shows model for basolateral OAT pathway.

hOAT1 interacts with more than a hundred compounds, and its substrates include endogenous compounds, such as dicarboxylates, cyclic nucleotides, prostaglandins, and urate as well as exogenous ones, such as drugs and environmental compounds (Sekine *et al.*, 2000). hOAT3 exhibits a wide substrate selectivity similar to hOAT1. OAT3 mediates the high-affinity transport of estrone sulfate, dicarboxylates and various drugs, even including the cationic drug cimetidine (Sekine *et al.*, 2006). The substrate specificities of hOAT1 and hOAT3 overlap, but hOAT1 has a larger contribution to low-molecular weight of hydrophilic organic anion as compared to hOAT3 that accepts more bulky amphiphatic anions (Tahara *et al.*, 2006).

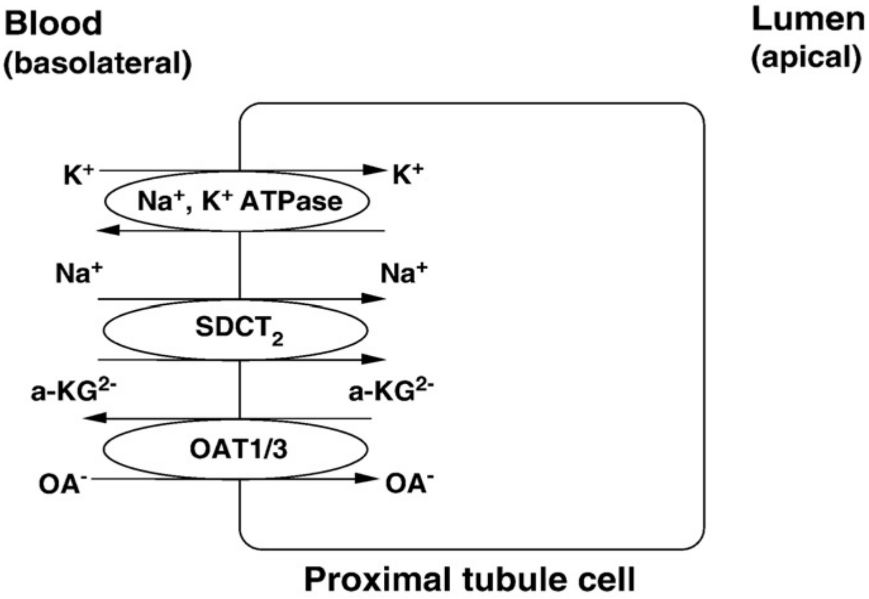
Blood
(basolateral)
Lumen
(apical)
K+
K+
Na+, K+ ATPase
Na+
Na+
SDCT2
a-KG2-
a-KG2-
OAT1/3
OA-
OA-
Proximal tubule cell

Figure 1.2 Model for basolateral OAT pathway. SDCT2: Na^+- coupled dicarboxylate cotransporter-2. OAT1/3: organic anion transporter 1 and 3. OA^-: organic anion (endogenous and exogenous anions). α-KG: α-ketoglutarate [Adapted from: Duan and You, 2010].

1.5 Organic anion transporter 1(OAT1/SLC22A6)

1.5.1 Biochemistry of hOAT1

OAT1 was the first organic anion transporter to be cloned and functionally characterized from human, monkey, pig, rabbit, rat and mouse (Buckhardt, 2012). Within the HUGO nomenclature, the gene for OAT1/Oat1 has been assigned the name SLC22A6 for humans and Slc22a6 for the other species. The mammalian OAT1 is composed of approximately 550 amino acids (aa) residues. In humans, four splice variants of hOAT1 (563, 550, 506 and 519 aa) occur in the kidney. The longer splice variants are hOAT1-1 and hOAT-2. hOAT1-1 is composed of 563 amino acids while hOAT1-2 is composed of 550 amino acids. The two shorter, non-functional splice variants are known as hOAT1-3 and hOAT1-4, respectively. The longer splice variants have identical transport functions while the shorter two have lack of transport capability (Bahn *et al.*, 2004).

The gene for human OAT1 is located on chromosome 11q12.3, near to the human OAT3 gene. Secondary structure of OAT1 consists of twelve putative transmembrane helices with nitrogen and carbon termini located at the cytosolic side of the plasma membrane, a large extracellular loop between transmembrane helices 1 and 2, and a large intracellular loop between helices 6 and 7 (Roth *et al.*, 2012). Moreover, the large extracellular loop between transmembrane helices 1 and 2 carries several glycosylation sites and the carbon terminus, whereas the intracellular loop between transmembrane helices 6 and 7 carry several consensus sequences for phosphorylation by protein kinases (Roth *et al.*, 2012).

Human OAT1 messenger RNA (mRNA) is strongly expressed in the kidneys (Bleasby *et al.*, 2006). Considerably low mRNA levels of hOAT1 are also found in brain, lung, skeletal muscles and stomach (Fromm and Kim, 2011).

Immunocytochemistry revealed that hOAT1 proteins are located at basolateral membrane of renal proximal tubule cells.. This location is consistent with the important role of hOAT1 in uptake of drugs from the blood into proximal tubule cells and may thus be regarded as a transporter specific to kidneys.

1.5.2 Structure and active site of hOAT1

As hOAT1 plays a significant role in handling of endogenous and exogenous organic anion by excretory and barrier tissues, the molecular level structure model of hOAT1 is the particular interest. Unfortunately, like other membrane proteins, there is a lack of structural information on OATs. Therefore, to overcome problems with protein crystallization, development of computational models to predict structure based on two-dimensional fold recognition between the target (a protein of unknown structure) and the template (a protein of known structure) is one of the emerging methods to create the homology model of the membrane protein (Perry *et al.*, 2006).

OATs share many structural features with major facilitator superfamily (MFS) proteins despite weak sequence similarities. MFS protein is one of the largest groups of secondary active transporters conserved from bacteria to humans (Yan, 2013). In particular, OATs possess MFS hallmark including 12 transmembrane α-helices with cytosolic nitrogen and carbon termini, a long intracellular loop that connects the two 6-helix halves, a sequence length between 400 and 600 amino acids, and a RXXXR signature sequence conserved between loop 2-3 (Maiden *et al.*, 1987; Pao *et al.*, 1998; Hirai *et al.*, 2004). Among the MFS proteins, X-ray crystal structure of glycerol 3-phosphate (GlpT, SLC37A2) and the lactose permease (LacY) of *Escherichia coli* are available and provide templates for OATs structure (Pelis *et al.*, 2011). GlpT (Protein Data Bank code 1pw4) was selected as a template for the hOAT1 model because

GlpT transports substrate as an antiporter was similar to the hOATs despite their low sequence identity (14%) (Perry *et al.*, 2006). A three-dimensional model of hOAT1 based on the structure of GlpT has been generated and illustrated in Figure 1.3.

According the study done by Perry and co-workers, the putative active site for hOAT1 was predicted and located in the cavity formed by the 12 transmembrane domains. The structural model of hOAT1 shows that helices 5, 7, 8, 10 and 11 surround an electronegative putative active site with a volume of ~830Å^3 (Perry *et al.*, 2006). This active site opens to the cytoplasm and is surrounded by residues Tyr230 (domain 5), Lys431 (domain 10) and Phe438 (domain 10). In addition, the residues Tyr230 and Phe438 have been identified as important amino acid residues in OAT1 substrate recognition and translocation based on the model and experimental mutations carried out (Perry *et al.*, 2006). Residue Arg466 is also one of the residues surround the putative active cavity of hOAT1 in the helix 11 and is a major determinant in substrate translocation (Rizwan *et al.*, 2007). Taken together, it appears that basic amino acid residues in trans-membrane helices 8, 10, and 11 play a role in dicarboxylate binding and these residues are Lys382 (domain 8), Lys431 (domain 10) and Arg466 (domain 11) (Kaufhold *et al.*, 2011).

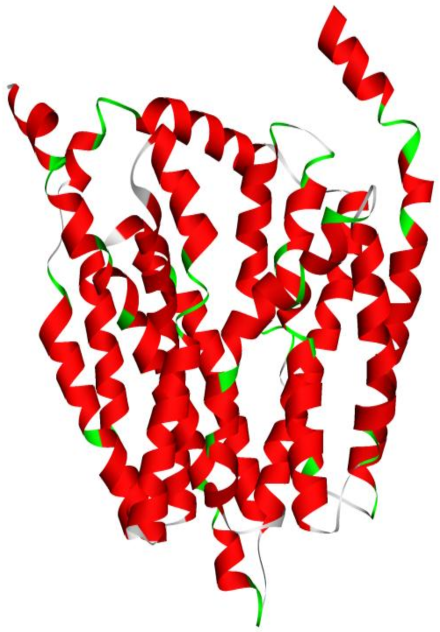

Figure 1.3 A three-dimensional model of hOAT1 based on the structure of GlpT. [Adapted from: Pelis *et al*., 2011]

1.5.3 Substrates of hOAT1

Under physiologic conditions, OAT1 are responsible as an antiporter exchanging intracellular α-ketoglutarate against extracellular organic anions and drugs. OAT1 is well-known for its very broad substrate specificity. The prototypical substrate to test heterologously expressed OAT1 *in vitro* is radiolabeled p-aminohippurate (PAH). Inhibition of PAH transport indicates an interaction of the tested compound with the investigated transporter, but does not necessarily implicate its transport (Burckhardt, 2012). Using various expression systems, the K_m value for PAH uptake by human OAT1 is ranged between 3.1 µM and 113 µM with a mean of 28.5 µM (Burckhardt, 2012). Furthermore, due to its broad substrate specificity, hOAT1 also is a key mediator in the distribution and renal tubular secretion of a multitude of endogenous substances, drugs and numerous active compounds from herbal medicines and food such as phenolic acids and flavonoids (Hong *et al.*, 2007; Wang and Sweet, 2012a). The substrates of hOAT1 is listed in Table 1.1.

1.5.4 Inhibitors of hOAT1

Inhibition of human OAT1 at the basolateral membrane of renal proximal tubule cells reduces the active tubular secretion of drugs. As a consequence, drug clearance is reduced and plasma drug concentrations of substrate drugs are elevated. Probenecid is the prototypical inhibitor of the OAT1 and OAT3 (Muller and Fromm, 2011). This drug was introduced in the 1950's to decrease the renal excretion and prolong the plasma half-life of penicillins (Cunningham *et al.*, 1981). The major route of the excretion of penicillin, renal tubular secretion is efficiently inhibited by probenecid. Meanwhile, it is also known that probenecid lowers serum uric acid concentrations and it has been used as uricosuric agent for the prevention of gout

Table 1.1 Compounds interacting with hOAT1

Compounds	**Substrates**	**Inhibitors**	**References**
Endogenous substances	• cGMP • Dicarboxylate α-ketoglutarate • Prostaglandin • Purine metabolite • Urine	• Dicarboxylate α-ketoglutarate • Urate	(Sekine *et al.*, 1997; Lu *et al.*, 1999; Kimura *et al.*, 2002; Sugawara *et al.*, 2005; Cropp *et al.*, 2008; Hagos *et al.*, 2008; Sato *et al.*, 2008)
ACE inhibitors	• Captopril • Quinapril	-	(Ueo *et al.*, 2007; Yuan *et al.*, 2009)
Angiotensin II receptor blockers	• Olmesartan	• Candesartan • Losartan • Pratosartan • Telmisartan • Valsartan	(Yamada *et al.*, 2007; Sato *et al.*, 2008)
Diuretics	• Bumetanide • Furosemide	• Loop diuretics • Bumetanide • Furosemide • Torasemide	(Hasannejad *et al.*, 2003; Bahn *et al.*, 2004; Hagos *et al.*, 2007)
Statins	• Fluvastatin • Simvastatin	-	(Takeda *et al.*, 2004; Windass *et al.*, 2007)
ß- lactam antibiotics	• Tetracyclines	• Tetracyclines • Cefazolin • Cefoperazone • Cefadroxil	(Babu *et al.*, 2002; Ueo *et al.*, 2005)